EMBO reports

scientific report

Dynamic interactions of a transcription factor with DNA are accelerated by a chromatin remodeller

Tatiana S. Karpova, Teresa Y. Chen, Brian L. Sprague & James G. McNally+
CCR Core Fluorescence Imaging Facility, Laboratory of Receptor Biology and Gene Expression, NCI, NIH, Bethesda, Maryland, USA

Most components in the nucleus are in a state of dynamic equilibrium maintained by the rapid mobility of nuclear proteins within and between compartments. Mobility is believed to reflect transient binding, but the identity of the binding sites and the function of the transient interactions are a matter of debate. Furthermore, we know little about how these processes may be regulated. Here, we investigate the nature and regulation of transcription factor binding and mobility in the nucleus of yeast cells. Using the Ace1p transcriptional activator, we show that nonspecific DNA binding interactions seem to have a role in retarding Ace1p nuclear mobility. Surprisingly, we find that this binding is a regulated process using a chromatin remodeller to speed up Ace1p interactions at nonspecific DNA sites. Our results suggest that transcription factor mobility represents a diffusion-driven, rapid sampling of nonspecific DNA sites, and that chromatin remodellers accelerate this genomic search process.

Keywords: FRAP; transcription; chromatin remodelling; nuclear mobility; DNA binding
EMBO reports (2004) **5**, 1064–1070. doi:10.1038/sj.embor.7400281

INTRODUCTION

As revealed by fluorescence recovery after photobleaching (FRAP), many proteins in the nucleus, including several transcription factors, are highly mobile. Although they move rapidly, these proteins do not move as fast as a freely diffusing molecule such as green fluorescent protein (GFP; Misteli, 2001). This implies that, similar to other nuclear proteins, transcription factors are retarded by binding interactions of some sort as they move through the nucleus. Several uncertainties remain to be clarified about this behaviour, including the identity of the binding sites and whether binding is specific or regulated.

Most of our knowledge of transcription factor mobility comes from steroid receptors, the mobility of which is known to require energy, proteasome function and molecular chaperones (Stenoien *et al*, 2001; Schaaf & Cidlowski, 2003; Elbi *et al*, 2004). Some evidence suggests that these transcription factors are normally bound to the nuclear matrix (Stenoien *et al*, 2001; Schaaf & Cidlowski, 2003), but other data argue against this (Sprague *et al*, 2004).

Here, we have used yeast molecular genetics to identify the natural binding state of a transcription factor, Ace1p, which is required in yeast for copper detoxification (Furst *et al*, 1988). The Ace1p protein has a simple domain structure that allows a direct test of how DNA binding contributes to nuclear mobility. In addition, by mutating other cellular factors, we have investigated how mobility of Ace1p is regulated. These studies suggest that Ace1p mobility corresponds to the rapid sampling of nonspecific DNA binding sites, and that a chromatin remodeller normally accelerates this process.

RESULTS AND DISCUSSION

Mobility is retarded by nonspecific DNA binding

Our carboxy-terminal fusion of GFP to Ace1p was functional. It rescued the copper sensitivity of the *ace1* knockout (data not shown), and localized to the nucleus (Fig 1A) consistent with Szczypka & Thiele (1989). FRAP recoveries for Ace1p–GFP were obtained using a 0.7-μm-diameter circular bleach spot (Fig 1B) positioned at random locations within the ~2-μm-diameter diploid yeast nucleus. The fusion protein was overexpressed ~3-fold in these cells (~5,000 Ace1p–GFP molecules per nucleus), on the basis of measurements of known concentrations of GFP imaged under identical conditions. These relatively low levels and the small bleach spots used here necessitated averaging of ~20 or more data sets to produce reasonably smooth FRAP recovery curves for Ace1p–GFP (Fig 1C). The averaged FRAP curves were then fitted with models for FRAP recovery described by Sprague *et al* (2004). The fitting routine estimates the bleach depth by extrapolating back from the first time point at $t = 2$ ms. The fitted recovery curves are presented here (Fig 1D, and in all subsequent figures) with the bleach depth normalized to 0, and standard errors of the mean indicated at each time point.

FRAPs of Ace1p–GFP revealed rapid exchange typical of other transcription factors (McNally *et al*, 2000; Stenoien *et al*, 2001; Schaaf & Cidlowski, 2003). However, the Ace1p–GFP recovery was significantly slower than that of GFP alone (Fig 2A), predicting a mass of 1.4 MDa for Ace1p–GFP (see Methods), far in excess of the real mass (55 kDa). This suggests that Ace1p–GFP recoveries are retarded by binding interactions.

CCR Core Fluorescence Imaging Facility, Laboratory of Receptor Biology and Gene Expression, NCI, NIH, 41 Library Drive, Bethesda, Maryland 20892, USA
+Corresponding author. Tel: +1 301 402 0209; Fax: +1 301 496 4951;
E-mail: mcnallyj@exchange.nih.gov

Received 11 December 2003; revised 23 September 2004; accepted 23 September 2004; published online 22 October 2004

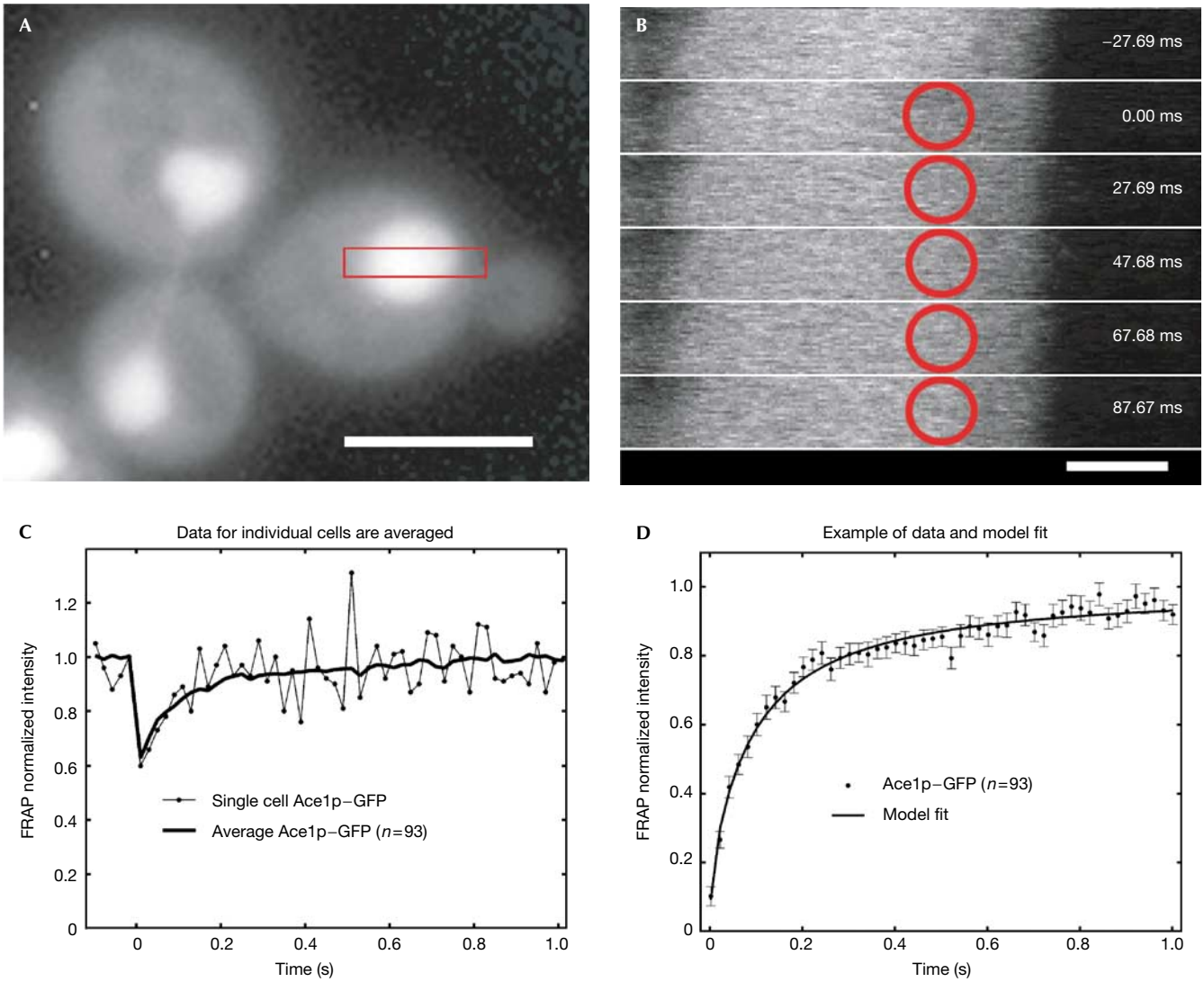

Fig 1 | Effective diffusion of Ace1p–GFP in the nucleus. (**A**) Nuclear localization of Ace1p–GFP fusion. Cells were imaged on a Leica DMRA microscope with a Photometrics SenSys camera (KAF1400 chip), 100 ×, 1.30 NA objective. Scale bar, 5 μm. (**B**) Cells were bleached with a 0.7-μm-diameter circular spot (red circle), and then images defined by the red rectangular box in (**A**) were recorded every 20 ms (the first five timepoints after the bleach are shown). At each time point, average intensity within the spot was measured. Scale bar, 1 μm. (**C**) Owing to the small bleach-spot size and the low expression levels, individual FRAP curves were noisy (thin line), but averaging of many FRAP recoveries (always >19) yielded a smoother curve (thick line). (**D**) These averaged curves were then normalized from 0 to 1, with standard errors at each time point shown. The data were well fitted with an effective diffusion model for FRAP recovery. The effective diffusion fit indicates a rapid diffusion-driven sampling of many binding sites during the FRAP recovery period. Here, and in the following figures, the numbers of cells analysed are in parentheses, FRAP data are indicated by dots and fits are indicated by lines.

By fitting a model for FRAP recoveries (Sprague *et al*, 2004) to the Ace1p–GFP FRAP data, we have quantitatively accounted for these binding interactions and defined the mechanism of Ace1p–GFP movement in the nucleus. The averaged Ace1p–GFP recoveries were well fitted by an effective diffusion model (Sprague *et al*, 2004) using a single parameter for recovery rate (Figs 1D,2A). In a FRAP recovery, effective diffusion arises when the time to associate with a binding site is much faster than the time to diffuse across the bleach spot. Therefore, during the time frame of the FRAP recovery, each Ace1p molecule is transiently bound at many sites, moving from one site to the next by simple diffusion. When binding interactions are altered in such a scenario, small changes in the FRAP curve result, essentially because the diffusive component of the curve has been unaffected (Fig 2B). Therefore, even small changes in the FRAP curves may indicate significant changes in binding.

To investigate sites for Ace1p binding, we removed its DNA binding domain (DBD; Brown *et al*, 2002). This mutant protein no longer localized to the nucleus, so we constructed a DBD^{-} nuclear localization signal (NLS) to ensure that FRAPs of the

DBD$^-$ mutant were performed in nuclei. For valid comparison, we also added an NLS to Ace1p–GFP and performed FRAPs of both the full-length and mutant proteins. The DBD$^-$ mutant recovered faster than the full-length protein (Fig 2C), demonstrating that Ace1p–GFP mobility is normally retarded by DNA binding.

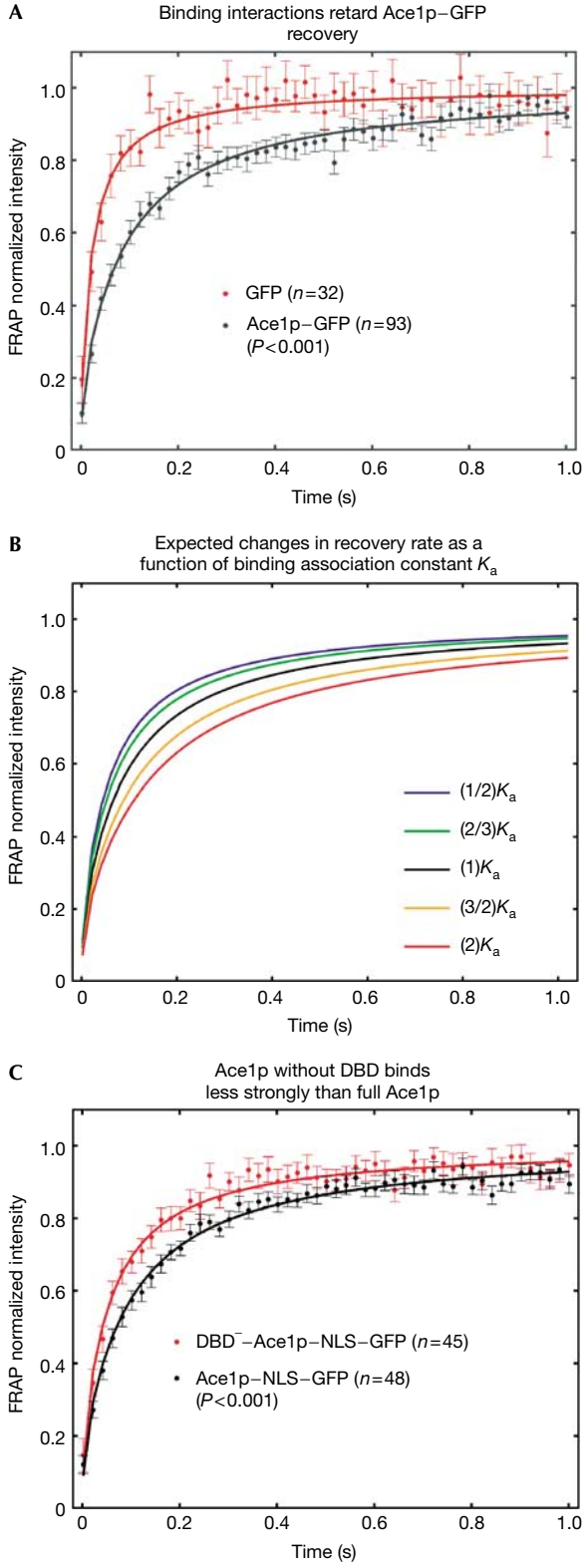

This DNA binding is likely to be nonspecific, as only a negligible fraction of the total Ace1p–GFP fluorescence throughout the nucleus can arise from binding at known specific sites. There are at most 32–64 Ace1p-specific sites in the yeast genome, and virtually all are clustered at the same amplified chromosomal locus CUP1 (Welch *et al*, 1983). We conclude that DNA is a target of Ace1p binding and that much of this binding is probably nonspecific.

Our FRAP analysis enables an *in vivo* estimate of a nonspecific DNA binding constant. Using the effective diffusion fit, and estimating a free DNA concentration of ~1–10 mM (see Methods), we obtain a range for the *in vivo* association constant $K_a \sim 10^2$–$10^3\,M^{-1}$. This is an order of magnitude estimate owing to the approximations made in FRAP modelling (see Methods) and our ignorance about the free DNA concentration in a live cell. The lower bound for K_a presumes that all DNA sites are accessible *in vivo*, whereas the upper bound presumes that only 10% of the sites are available, with the remainder masked by chromatin. To compare this estimate of K_a with typical *in vitro* values of nonspecific DNA binding, we must account for the presence of histones *in vivo*, which neutralize approximately half the DNA charge (Clark & Kimura, 1990). Here an order-of-magnitude estimate predicts that K_a *in vivo* should be approximately the square root of K_a *in vitro* (see Methods). As the *in vitro* data for nonspecific DNA binding range from 10^4 to $10^5\,M^{-1}$ (Oda & Nakamura, 2000), they are consistent with our *in vivo* estimate of 10^2–$10^3\,M^{-1}$ for Ace1p nonspecific DNA binding.

Regulation of mobility by a chromatin remodeller

To test if Ace1p nonspecific DNA binding was regulated, we investigated chromatin remodellers. Several *in vitro* studies as well as an *in vivo* chromatin immunoprecipitation analysis have suggested that chromatin remodellers can displace transcription factors from specific DNA binding sites (Fletcher *et al*, 2002; Kassabov *et al*, 2002; Moreau *et al*, 2003; Nagaich *et al*, 2004). To test an *in vivo* role for chromatin remodellers at nonspecific DNA sites, we performed FRAPs of Ace1p–GFP in disruption mutants for different remodellers: *swi2*Δ (an ATPase of the SWI/SNF complex; Cairns *et al*, 1994; Cote *et al*, 1994); *rsc1*Δ, *rsc2*Δ (subunits of the RSC1 and RSC2 complexes; Cairns *et al*, 1996, 1999); *rad54*Δ (an ATPase with chromatin-remodelling activity; Alexeev *et al*, 2003); *isw1*Δ, *isw2*Δ (ATPases of ISWI1 and ISWI2 complexes; Tsukiyama *et al*, 1999); and *chd1*Δ (an ATPase of CHD/Mi2 complex; Tran *et al*, 2000).

◀ **Fig 2** | Ace1p–GFP recoveries are retarded by DNA binding. (**A**) In comparison with unconjugated GFP, the Ace1p recovery is significantly slower, implicating binding interactions. (**B**) A family of predicted FRAP recovery curves for effective diffusion. These curves were obtained by varying the binding association constant, $K_a = k_{on}/k_{off}$, holding cellular diffusion (D_{GFP}) constant. (**C**) FRAP recoveries for Ace1p lacking the DNA binding domain (DBD$^-$) were significantly faster than the full protein, demonstrating that DNA binding normally retards the recovery. *P*-values shown here and in subsequent plots are calculated on the basis of the fitted FRAP recovery rates determined by the effective diffusion constant (see Methods).

In most disruption mutants (Fig 3), FRAP recoveries of Ace1p–GFP were not significantly different from wild type, with the exception of *rsc2*Δ, where we were able to detect a significant slowdown (Fig 4A). This slowdown was not due to a global change in nuclear structure or mobility arising in *rsc2*Δ, because GFP nuclear recoveries were unaffected in the *rsc2*Δ strain (Fig 4B). Interestingly, slower Ace1p–GFP recoveries did not occur after loss of the related RSC1 complex (Figs 4C and 3F). The RSC1 complex differs from the RSC2 complex in only one subunit (Rsc1p replaces Rsc2p), and the two complexes bind to many of the same sites (Ng *et al*, 2002). Our FRAP data therefore suggest a highly specific role for Rsc2p.

In principle, chromatin-remodelling activity could influence transcription factor mobility by several mechanisms. The absence of a remodeller should decrease the accessibility of nucleosomal DNA (Längst & Becker, 2001), thereby reducing the average 'on' rate of a transcription factor to DNA. Because $K_a = k_{on}/k_{off}$, a reduced k_{on} should yield a reduced K_a. However, fits to our FRAP data reveal the opposite, with K_a increasing by 1.6-fold in *rsc2*Δ. To account for this increase, any decrease in k_{on} must therefore be compensated for by an even larger decrease in k_{off}. This is in fact consistent with the proposed role of remodellers in catalysing removal of transcription factors from DNA sites (Fletcher *et al*, 2002; Kassabov *et al*, 2002; Moreau *et al*, 2003; Nagaich *et al*, 2004). Thus, RSC2 may normally interact directly with Ace1p and catalyse its removal from nonspecific sites. However, an indirect interaction is also possible. As this remodeller is relatively abundant in yeast (Cairns *et al*, 1996), it may bind at a multitude of genomic sites and inadvertently disrupt transcription factors bound nonspecifically in its vicinity.

In either of these two scenarios, the decreased mobility of Ace1p seen in the absence of a specific remodeller may reflect genome-wide remodelling action, as suggested by recent studies demonstrating the widespread distribution of remodellers beyond promoter sites (Ng *et al*, 2002). Increased mobility of Ace1p would then be a consequence of this global remodelling action, a phenomenon that could have functional significance. Our data suggest that Ace1p nuclear mobility reflects the rapid, diffusion-driven sampling of nonspecific DNA binding sites. This supports the general hypothesis that nuclear protein mobility represents the process of genome-wide search for specific target sites (Phair *et al*, 2004). Our observations not only suggest that this is what Ace1p nuclear mobility reflects but also show that a chromatin remodeller can accelerate this sampling process.

METHODS

Strains and plasmids. Wild type and strains homozygous for disruptions of *swi2*, *rsc1*, *rsc2*, *isw1*, *isw2*, *rad54* and *chd1* were diploids in the BY4743 genetic background isogenic to the SC288C strain (Research Genetics/Invitrogen, Huntsville, AL, USA). Each strain was transformed with either pTSK65 (Ace1p–GFP), pTSK288 (Ace1p–GFP–NLS), pTSK119 (transcriptional activation domain (TAD)–GFP–NLS), pTSK20 (GFP) or pTSK136 (GFP–NLS). To ensure nuclear retention, we added in some cases an NLS to certain constructs, as indicated above. Autonomous plasmids were constructed from the vector p2HG/N792 carrying the yeast constitutive *GPD* promoter, *HIS3* marker and 2 μm plasmid replicator (a gift from Dr S. Lindquist, Whitehead Institute, Cambridge, MA, USA). To construct pTSK65, two fragments were inserted into the vector p2HG/N792: (1) the yeast *ACE1* gene that was PCR amplified from genomic DNA using primers CATG *GGATCC* cgaataaacacacataaataaacaaa ATGGTCGTAATTAACG GGGT (*GPD* leader sequence in small letters, *Bam*HI site in italics) and CCGA*GCGGCCGC* TTGTGAATGTGAGTTATGCGA (*Not*I site in italics); (2) the yeast-enhanced GFP (Cormack *et al*, 1997) that was PCR amplified from pBM3412 (a gift from Dr M. Johnston, Washington University, St Louis, MO, USA) using primers CATG *GCGGCCGCC* gctgctgccgctgcagctgctgcagctgcg ATGTCTAAAGGTGAAGAATTATTC (13-ala protein linker in small letters, *Not*I site in italics) and CCGA *CCGCGG* TTATTTG TACAATTCATCCATACCATGGGT (*Sac*II site in italics).

To construct pTSK119, a C-terminal fusion of GFP to the TAD of the *ACE1* gene was PCR amplified from pTSK65 using primers CATG *GGATCC* atg AAGGGAGGGTCATGCCACAGAAGG (*Bam*HI site in italics, added ATG codon in small letters) and CCGA *CCGCGG* TCATCA ggcaacctttctcttcttctttggtggagt TTTGTA CAATTCATCCATACCATGGG (NLS in small letters, *Sac*II site in italics) and inserted into pTSK65.

To construct pTSK136, GFP was PCR amplified from pBM3412 using primers CATG *GGATCC* cgaataaacacacataaataaacaaa ATGTCTAAAGGTGAAGAATTATTC (*GPD* leader sequence in small letters, *Bam*HI site in italics) and CCGA *CCGCGG* TCATCA ggcaacctttctcttcttctttggtggagt TTTGTACAATTCATCCATACCAT GGG (NLS in small letters, *Sac*II site in italics) and inserted into pTSK65.

To construct pTSK20, GFP was PCR amplified from pBM3412 using primers CATG *GGATCC* cgaataaacacacataaataaacaaa ATGTCTAAAGGTGAAGAATTATTC (*GPD* leader sequence in small letters, *Bam*HI site in italics) and CCGA *GCGGCCGC* AGCAGCTGCAGCAGCTGCAGCGGCAGCAGCTTTGTACAATTC ATCCATACCATGGGT (*Not*I site in italics) and inserted into p2HG/N792 to replace the glucocorticoid receptor.

To construct pTSK288, GFP–NLS fragment was cut out of pTSK119 (*Not*1–*Sac*II) and inserted into pTSK65 to replace GFP.

Microscopy and FRAP. Cultures were grown at 28 °C in CSM–histidine (complete supplement mixture, Bio101 Inc., Vista, CA, USA). Overnight cultures were diluted 1:30 in fresh CSM–histidine and grown for 3–6 h. Cells were concentrated from 500 μl of the culture by centrifugation. Drops (2 μl) were placed on a slide and covered with coverslips.

FRAP experiments were carried out on a Zeiss 510 confocal microscope with a 100× and 1.3 NA oil immersion objective. Cells were imaged with a 488 nm laser line from a 40 mW argon laser at low laser intensity (0.75%) to reduce bleaching due to imaging. Bleaching was performed with the 488 nm line operating at 75% laser power. A single iteration was used for the bleach pulse, which lasted 7 ms. The measured diameter of the bleach spot was 0.7 μm. Fluorescence recovery was monitored every 20 ms. All the experiments were repeated at least twice. The total cell number analysed for each experiment was routinely more than 19. For each data set shown, separate FRAPs were performed and then averaged to generate a single FRAP curve.

FRAP analysis. Averaged FRAP curves were fitted with a routine that estimates the bleach depth, the recovery rate and the immobile fraction. The immobile fraction for Ace1p–GFP varied from day to day, but was always less than 3%. Bleach depths also varied from day to day, presumably owing to variations in laser power or transmittance. Owing to the variation in these

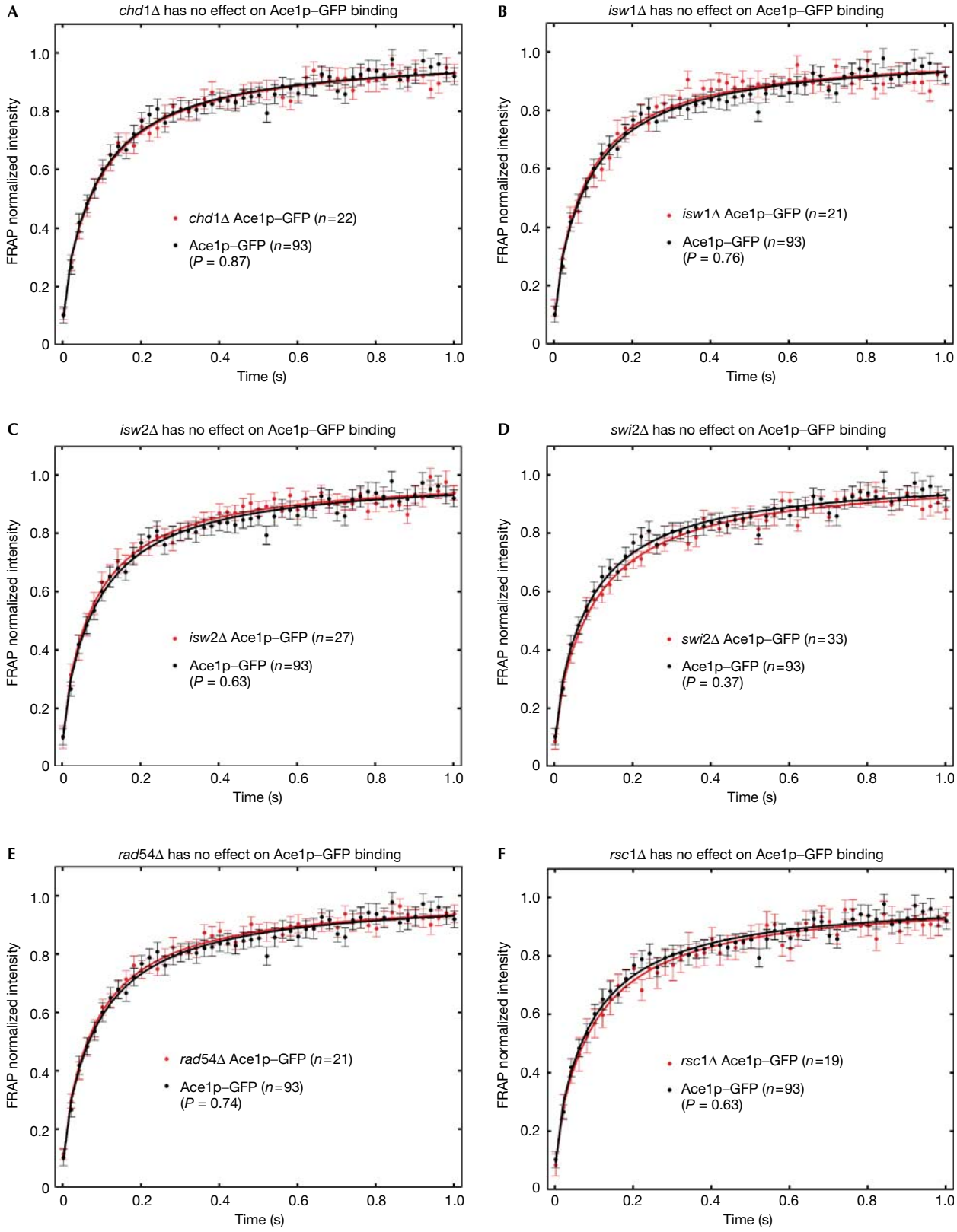

Fig 3 | Most remodellers do not significantly influence Ace1–GFP FRAP recoveries. FRAP recovery rates of Ace1p–GFP were not significantly altered after disruption of any of the chromatin remodellers indicated.

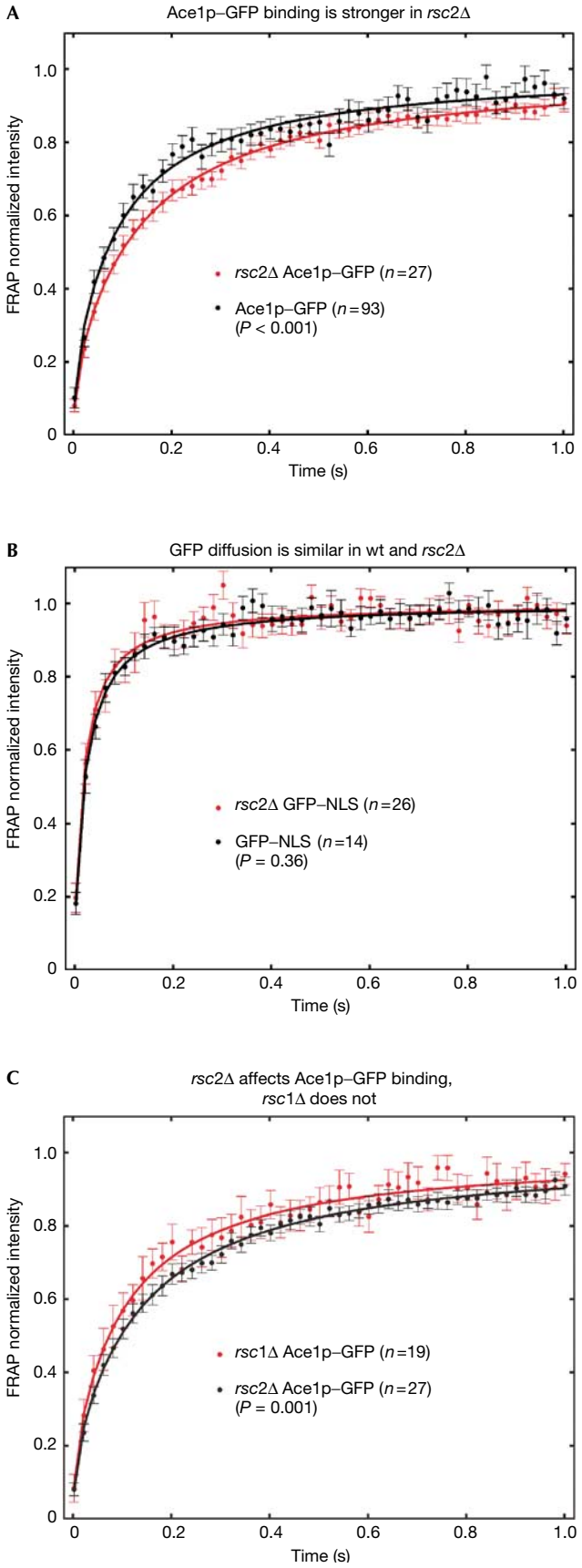

parameters, FRAP curves were compared on the basis of the recovery rate. This is determined by all of the FRAP data points, and as described below can be captured for Ace1p–GFP in a single parameter, namely the effective diffusion constant.

The FRAP fits presume a homogeneous distribution of binding sites photobleached with a cylindrical bleach pattern. These conditions are only approximately met in real cells, so the resultant estimates of binding parameters are themselves approximations.

To apply the method described by Sprague *et al* (2004), we first measured FRAPs with different spot sizes and detected different recovery curves, demonstrating that diffusion contributed to the recovery. Consistent with this, recoveries were well fitted by the effective diffusion approximation, and this fit was in turn consistent with an independent fit using the full model (Sprague *et al*, 2004). Fits were performed with the *nlinfit* routine in Matlab (The Math Works Inc., Natick, MA, USA), which for each fit yielded a standard error estimate on the parameter, essentially the effective diffusion constant, which describes recovery rate for the curve. These standard errors were in turn used to compute *P*-values for curve comparisons.

The effective diffusion constant predicted by these fits ($D_{ACE1-GFP}$) was significantly smaller than the free diffusion constant determined for unconjugated GFP (D_{GFP}). As $D \propto M^{-1/3}$, where M is the mass, $D_{ACE1-GFP}/D_{GFP} = (M_{ACE1-GFP}/M_{GFP})^{-1/3}$. This yields a large estimate (1.4 MDa) for the mass of ACE1p–GFP, presuming no binding interactions. Therefore, the slowed recovery is more likely to be due to rapid binding interactions, as described by the process of effective diffusion.

To estimate association constants, we used the effective diffusion relationship (Sprague *et al*, 2004)

$$D_{ACE1-GFP} = D_{GFP}/(1 + K_a S_{eq}) \quad (1)$$

where $K_a = k_{on}/k_{off}$ is the association constant of binding and S_{eq} is the equilibrium concentration of free binding sites. A range of 1–10 mM for S_{eq} was estimated by calculating the molar concentration for 2.5×10^7 base pairs of DNA in a diploid nucleus of 1 μm radius, assuming that either all or only 10% of sites are accessible. This enables an estimate of K_a using both equation (1) and the values obtained for $D_{ACE1-GFP}$ and D_{GFP} from the FRAP fits.

To generate the curves in Fig 2A, we varied K_a in equation (1) to yield different values for $D_{ACE1-GFP}$. For each $D_{ACE1-GFP}$, we calculated $\tau_D = w^2/D_{ACE1-GFP}$, where $w = 0.35$ μm is the bleach-spot radius. Each τ_D was then used in equation (16) from Soumpasis (1983) to compute a predicted FRAP recovery curve (see also equations (7) and (8) in Sprague *et al*, 2004).

Comparison of K_a values for nonspecific DNA binding. To compare the estimated *in vivo* K_a with the *in vitro* K_a, we used the relationship for DNA binding $d(\log K_a)/d(\log c) = -N$, where c

◀ **Fig 4** | RSC2 is required to accelerate Ace1p–GFP recoveries. (**A**) In an *rsc2*Δ strain, Ace1–GFP recoveries were significantly slower. (**B**) Recoveries of GFP alone were not significantly affected by loss of Rsc2, demonstrating that the observed slowdowns of Ace1p–GFP did not arise from a global change in nuclear mobility. (**C**) High specificity for Rsc2p is shown by comparison with the closely related RSC1 complex in which Rsc1p replaces Rsc2p. Loss of Rsc2p significantly alters recoveries, whereas loss of Rsc1p does not (see also Fig 3).

is the salt concentration of the surrounding milieu and *N* is the number of salt ions released from DNA on transcription factor binding (Manning, 1978). If, *in vivo*, histones neutralize approximately half the DNA charge (Clark & Kimura, 1990), then the number of salt ions released on transcription factor binding *in vivo* will be *N*/2 instead of *N*. Assuming that *c*, the salt concentration, does not change appreciably from *in vivo* to *in vitro*, then the factor of 1/2 in *N* must arise from a change in K_a. Given the logarithmic relationship above, this implies that (K_a *in vivo*) = (K_a *in vitro*)$^{1/2}$.

ACKNOWLEDGEMENTS

We thank D. Clark, C. Smith and D. Rau for advice, and S. Lindquist and M. Johnston for the vector plasmids.

REFERENCES

Alexeev A, Mazin A, Kowalczykowski SC (2003) Rad54 protein possesses chromatin-remodeling activity stimulated by the Rad51-ssDNA nucleoprotein filament. *Nat Struct Biol* **10:** 182–186

Brown KR, Keller GL, Pickering IJ, Harris HH, George GN, Winge DR (2002) Structures of the cuprous-thiolate clusters of the Mac1 and Ace1 transcriptional activators. *Biochemistry* **41:** 6469–6476

Cairns BR, Kim YJ, Sayre MH, Laurent BC, Kornberg RD (1994) A multisubunit complex containing the *SWI1/ADR6, SWI2/SNF2, SWI3, SNF5*, and *SNF6* gene products isolated from yeast. *Proc Natl Acad Sci USA* **91:** 1950–1954

Cairns BR, Lorch Y, Li Y, Zhang M, Lacomis L, Erdjument-Bromage H, Tempst P, Du J, Laurent B, Kornberg RD (1996) RSC, an essential, abundant chromatin-remodeling complex. *Cell* **87:** 1249–1260

Cairns BR, Schlichter A, Erdjument-Bromage H, Tempst P, Kornberg RD, Winston F (1999) Two functionally distinct forms of the RSC nucleosome-remodeling complex, containing essential AT hook, BAH, and bromodomains. *Mol Cell* **4:** 715–723

Clark DJ, Kimura T (1990) Electrostatic mechanism of chromatin folding. *J Mol Biol* **211:** 883–896

Cormack BP, Bertram G, Egerton M, Gow NA, Falkow S, Brown AJ (1997) Yeast-enhanced green fluorescent protein (yEGFP) a reporter of gene expression in *Candida albicans*. *Microbiology* **143:** 303–311

Cote J, Quinn J, Workman JL, Peterson CL (1994) Stimulation of GAL4 derivative binding to nucleosomal DNA by the yeast SWI/SNF complex. *Science* **265:** 53–60

Elbi C, Walker DA, Romero G, Sullivan WP, Toft DO, Hager GL, DeFranco DB (2004) Molecular chaperones function as steroid receptor nuclear mobility factors. *Proc Natl Acad Sci USA* **101:** 2876–2881

Fletcher TM, Xiao N, Mautino G, Baumann CT, Wolford R, Warren BS, Hager GL (2002) ATP-dependent mobilization of the glucocorticoid receptor during chromatin remodeling. *Mol Cell Biol* **22:** 3255–3263

Furst P, Hu S, Hackett R, Hamer D (1988) Copper activates metallothionein gene transcription by altering the conformation of a specific DNA binding protein. *Cell* **55:** 705–717

Kassabov SR, Henry NM, Zofall M, Tsukiyama T, Bartholomew B (2002) High-resolution mapping of changes in histone–DNA contacts of nucleosomes remodeled by ISW2. *Mol Cell Biol* **22:** 7524–7534

Längst G, Becker PB (2001) Nucleosome mobilization and positioning by ISWI-containing chromatin-remodeling factors. *J Cell Sci* **114:** 2561–2568

Manning GS (1978) The molecular theory of polyelectrolyte solutions with applications to the electrostatic properties of polynucleotides. *Q Rev Biophys* **2:** 179–246

McNally JG, Müller WG, Walker D, Wolford R, Hager GL (2000) The glucocorticoid receptor: rapid exchange with regulatory sites in living cells. *Science* **287:** 1262–1265

Misteli T (2001) Protein dynamics: implications for nuclear architecture and gene expression. *Science* **291:** 843–847

Moreau JL, Lee M, Mahachi N, Vary J, Mellor J, Tsukiyama T, Goding CR (2003) Regulated displacement of TBP from the PHO8 promoter *in vivo* requires Cbf1 and the Isw1 chromatin remodeling complex. *Mol Cell* **11:** 1609–1620

Nagaich AK, Walker DA, Wolford R, Hager GL (2004) Rapid periodic binding and displacement of the glucocorticoid receptor during chromatin remodeling. *Mol Cell* **14:** 163–174

Ng HH, Robert F, Young RA, Struhl K (2002) Genome-wide location and regulated recruitment of the RSC nucleosome-remodeling complex. *Genes Dev* **16:** 806–819

Oda M, Nakamura H (2000) Thermodynamic and kinetic analyses for understanding sequence-specific DNA recognition. *Genes Cells* **5:** 319–326

Phair RD, Scaffidi P, Elbi C, Vecerova J, Dey A, Ozato K, Brown DT, Hager G, Bustin M, Misteli T (2004) Global nature of dynamic protein–chromatin interactions *in vivo*: three-dimensional genome scanning and dynamic interaction networks of chromatin proteins. *Mol Cell Biol* **24:** 6393–6402

Schaaf MJ, Cidlowski JA (2003) Molecular determinants of glucocorticoid receptor mobility in living cells: the importance of ligand affinity. *Mol Cell Biol* **23:** 1922–1934

Soumpasis DM (1983) Theoretical analysis of fluorescence photobleaching recovery experiments. *Biophys J* **41:** 95–97

Sprague BL, Pego RL, Stavreva DA, McNally JG (2004) Analysis of binding reactions by fluorescence recovery after photobleaching. *Biophys J* **86:** 3473–3495

Stenoien DL, Patel K, Mancini MG, Dutertre M, Smith CL, O'Malley BW, Mancini MA (2001) FRAP reveals that mobility of oestrogen receptor-alpha is ligand- and proteasome-dependent. *Nat Cell Biol* **3:** 15–23

Szczypka MS, Thiele DJ (1989) A cysteine-rich nuclear protein activates yeast metallothionein gene transcription. *Mol Cell Biol* **9:** 421–429

Tran HG, Steger DJ, Iyer VR, Johnson AD (2000) The chromo domain protein Chd1p from budding yeast is an ATP-dependent chromatin-modifying factor. *EMBO J* **19:** 2323–2331

Tsukiyama T, Palmer J, Landel CC, Shiloach J, Wu C (1999) Characterization of the imitation switch subfamily of ATP-dependent chromatin-remodeling factors in *Saccharomyces cerevisiae*. *Genes Dev* **13:** 686–697

Welch JW, Fogel S, Cathala G, Karin M (1983) Industrial yeasts display tandem gene iteration at the CUP1 region. *Mol Cell Biol* **3:** 1353–1361